J Therm Anal Calorim (2015) 120:1543–1551
DOI 10.1007/s10973-015-4482-7

Thermal and structural characterization of ultrasonicated Bi–Sn alloy in the eutectic composition

Martina Pilloni · Guido Ennas · Valentina Cabras · Valeria Denotti · Vijay Bhooshan Kumar · Anna Musinu · Ze'ev Porat · Alessandra Scano · Aharon Gedanken

Received: 19 November 2014 / Accepted: 23 January 2015 / Published online: 18 February 2015

Abstract Irradiation of the molten eutectic $Bi_{43}Sn_{57}$ alloy with ultrasonic energy produced different bismuth–tin phases that were not reported in the equilibrium binary phase diagram. The X-ray powder diffraction data, refined using the Rietveld method, allowed the identification of these metastable phases and their crystal structure. The Bi_2Sn and β′-Sn phases, with distorted β-Sn type structure, were obtained in the sample which was rapidly quenched after ultrasonication. On the other hand, the equiatomic phase BiSn was obtained in the quenched sample when the ultrasonication was continued during the rapid cooling below the eutectic point. The ultrasonicated samples were characterized by differential scanning calorimetry. The results suggested that the metastable phases, which were kinetically stable at RT, decomposed into equilibrium components during the heating treatment at 320 °C, and that this conversion is an irreversible process. Observations by scanning electron microscopy and energy dispersive X-ray analysis complete the characterization of samples.

Keywords Sonochemistry · Eutectic binary bismuth–tin alloy · Metastable alloy · Lead-free alloy

M. Pilloni (✉) · G. Ennas · V. Cabras · V. Denotti · A. Musinu · A. Scano
Dipartimento di Scienze Chimiche e Geologiche, Università di Cagliari, Cittadella Universitaria Monserrato, 09042 Monserrato, CA, Italy
e-mail: martina.pilloni@unica.it

V. B. Kumar · A. Gedanken
Department of Chemistry, Bar-Ilan University, 52900 Ramat Gan, Israel

Z. Porat
Institute of Applied Research, Ben-Gurion University of the Negev, 84105 Beersheba, Israel

Z. Porat
Division of Chemistry, Nuclear Research Center-Negev, P.O. Box 9001, 84190 Beersheba, Israel

A. Gedanken
Department of Materials Science and Engineering, National Cheng Kung University, Tainan 70101, Taiwan

Introduction

At atmospheric pressure, the bismuth–tin system has a simple eutectic binary phase diagram, in which Sn dissolves approximately 10 mass% of Bi at the eutectic temperature [1, 2]. The eutectic alloy ($Bi_{43}Sn_{57}$, atomic composition) consists of tetragonal tin phase (β-Sn) and bismuth phase. It is well known that the behavior of this system is modified under high pressure (in the GPa order) and that metastable Bi_xSn_{1-x} structures may be obtained [3]. In the past decades, a wide literature discussed about the formation and the nature of the metastable phases of Bi–Sn and a metastable phase diagram was conducted [4]. The formation of metastable Bi–Sn solid solution was achieved simply by a considerable undercooling of the melt [5] or by applying high pressure together with rapid quenching [4, 6] In some cases, the metastable phase decomposed into the equilibrium components in the range of −40 to 100 °C [7]. Although different approaches for rapid solidification were proposed in recent years [8], traditionally the melt quenching is the method more frequently adopted for undercooling the alloys. The main practical problem encountered in the use of rapid quenching is the difficulty to achieve the high cooling rate (generally 10^5–10^6 K s^{-1}). Furthermore, using traditional methods the resulting products are often large sized, such

as the ribbons obtained in previous works with width of 3 mm and thickness of 60–80 μm [9].

Different methods have been developed to prepare metal alloys, including mechanical alloying [10] deposition processes [11, 12] and chemical reduction [13]. In addition, the sonochemical method is a very promising way to obtain nanoparticles of alloys and other unusual materials [14, 15]. Irradiation of a liquid with high-intensity ultrasonic energy induces acoustic cavitation process that includes formation, growth and collapse of gas bubbles. The rapid collapse of these gas bubbles creates extreme local conditions of high temperatures (ca. 5,000 K) and pressure (ca. 1,000 atm) and cooling rates above 10^{10} K s^{-1} [16]. It was reported that melting some low-melting point metals, such as Sn, Bi Pb and others in silicone oil, followed by ultrasonic irradiation, caused the dispersion of the molten metals into micron-size stable spheres [17]. Recently, this method was applied to several binary combinations of molten bismuth with one of other low-melting point metals (Sn, In, Ga and Zn), and in all cases, microspheres of various structures and compositions were obtained [18].

This work presents the results of the ultrasonic irradiation of molten BiSn alloy having a eutectic composition. Two different experiments were carried out to explore the combined effect of sonication and cooling on the structure of the solidified alloy. The samples were characterized by X-ray powder diffraction (XRPD), differential scanning calorimetry (DSC), scanning electron microscopy (SEM) and energy dispersive X-ray analysis (EDAX). The X-ray diffraction data were simulated by the Rietveld refinement method in order to define the composition of Bi–Sn non-equilibrium phases.

Experimental

Tin foil (0.127 mm thickness; 99.9 % purity) and granulated bismuth (99 % purity) were purchased from Aldrich and used as starting material. Bi–Sn alloy in the eutectic composition (εBi–Sn) was prepared by melting together 2.1506 g of Sn and 2.901 g of Bi in a graphite crucible and casting of the melt. Acetone used for washing the products was of analytical grade (ACS reagent) purchased from J.T. Baker.

Synthesis of sample 1

A portion (0.4 g) of the eutectic alloy was transferred into a test tube (7.5 cm long, 2.5 cm in diameter) containing 4 mL of silicone oil [Wacker Silicone oil AP 150, Fluka (150 mPa, neat (25 °C))]. The test tube was dipped in a temperature-controlled oil bath and heated at 154 °C to melt the sample. The horn of an ultrasonic transducer was dipped in the test tube, ca. 1.5 cm above the molten alloy, and the system was irradiated at 23 kHz for 3 cycles of 10 s sonication and 10 s rest. A gray suspension of particles was formed in the oil which was immediately quenched down to 110 °C by adding fresh silicon oil into bath. After cooling to RT (with an average rate of 2 °C min^{-1}), the particles were separated by centrifugation, washed with acetone and separated again by centrifugation. This procedure was repeated several times to completely remove the silicone oil.

Synthesis of sample 2

This sample was prepared according to the same procedure as the previous one; however, the sonication was continued, while the sample was cooled to 110 °C (at an average rate of 15 °C s^{-1}) for another 60 cycles. After cooling to room temperature, the particles were separated and washed as described above.

Structural and morphological characterizations

A Seifert X3000 apparatus in the Bragg–Brentano geometry was used for X-Ray Powder Diffraction. It was operated using the CuK_α radiation in the range of 10°–80° (2θ degrees) with step of 0.05°, a counting time of 36 s per step and with an opportune counting time to optimize the signal/noise ratio. Rietveld structural refinement was performed using Maud software [19, 20] to evaluate several parameters: phases contents, lattice parameter, average crystalline size and microstrain. Environmental scanning electron microscopy (ESEM) was performed using an Inspect FEI microscope at 20 keV. The samples, which were dried in a glove box, were applied on a sample holder coated with a carbon tape and then coated with a carbon layer to improve conductivity. The composition of the samples was determined by using energy dispersive X-ray spectroscopy (EDS).

Thermal characterization

Differential scanning calorimetry (DSC) measurements were performed at atmospheric pressure using a Perkin Elmer instrument model DSC7. The measurements were performed under Ar flow (60 mL min^{-1}). Samples of 5 mg were encapsulated in aluminum crucibles and scanned with consecutive thermal cycles in the temperature range of 20–320 °C with a heating rate of 10 °C min^{-1}. The temperature of the invariant phase reaction (eutectic temperature, T_e) was taken from the extrapolated temperature on the onset of the corresponding peak on heating [1].

Within the range of temperatures investigated (20–320 °C), thermal treatments at intermediate temperatures are carried

out on samples. These treatments were performed in Ar flow with a heating rate of 10 °C min^{-1} and cooling rate of 200 °C min^{-1}.

Results and discussion

SEM images of the particles that were obtained by the two synthetic procedures are presented in Fig. 1. In both cases, the particles are spherical, in the sub-micrometer scale, but the average particles size seems to be somewhat smaller for sample 2 (Fig. 1b). This may be due to the much longer sonication duration that this sample has experienced. EDS elemental analysis shows the presence of solely Bi and Sn; for sample 1, the atomic ratio is 41.5:58.5 %, respectively, and for the sample 2, it is 43.1:56.9. Both these ratios are close to the eutectic composition, thus showing that the melts have undergone no compositional change upon the ultrasonic irradiation, but a reduction on average particles size is observed.

Dried samples of the two samples were examined by X-ray diffraction. The XRPD pattern for sample 1 is presented in Fig. 2: the main Bragg reflections match with the database values for the Sn and Bi phases. In addition, peaks at 28.75, 41.05, 42.40 and 43.50° (2θ degrees) were also observed. It is noteworthy that the Sn diffraction peaks at 30.60, 32.00, 43.80 and 44.90° (2θ degrees), assigned to (200) (101), (220) and (211) lattice planes, respectively, appear split. These observations suggest that in sample 1, the Sn and the Bi phases coexist with other metastable phases. No peaks ascribable to metal oxide were found which means that no oxidation of the metals took place during the sonication process.

The Rietveld refinement procedure was applied to the X-ray diffraction data in order to obtain the phase composition, the lattice parameters, the average crystallite size and the microstrain (σ) for each of the phases present in sample 1. The results are presented in Table 1 together with those related to sample 1 treated at 320 °C. The results show for sample 1 that the main phases are the tetragonal structure of Sn (β-tin) and the rhombohedral structure of Bi. This indicates that the Bi–Sn alloy which rapidly solidified from the sonicated melt is partially of the eutectic composition. As expected for this binary system, the solidification of the eutectic melt gives rise to a heterogeneous alloy in which the equilibrium phases are bismuth and tin. While the solubility of Sn in Bi is negligible, the Sn component dissolves approximatively 10 mass% of Bi at the eutectic temperature [1]. As the alloy cools, the solubility of bismuth decreases and the atoms precipitate

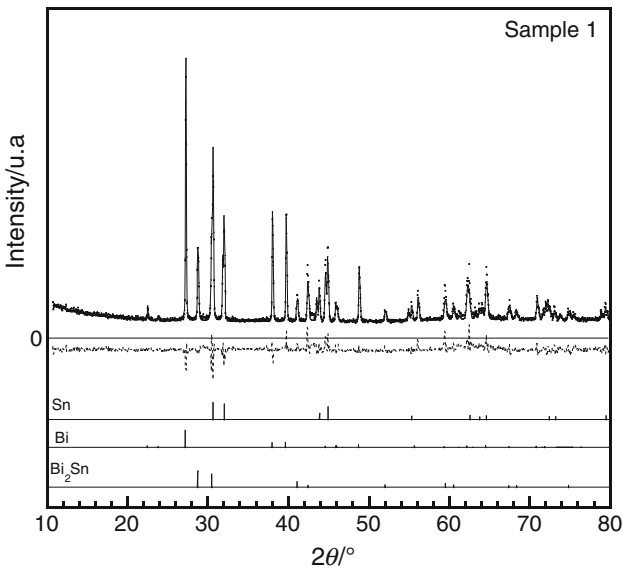

Fig. 2 Rietveld plot for sample 1. The dots are the experimental data, the *solid line* is the calculated data and the *dotted line* shows the difference profile. The *lower vertical bars* represent reflection positions of Bi (PDF card 44-1246), Sn (PDF card 04-0673) and Bi_2Sn phases

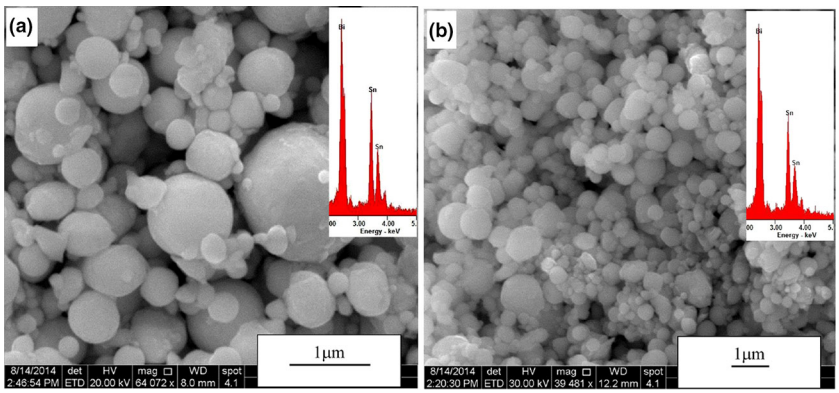

Fig. 1 SEM images of the two samples. **a** Sample 1, in which quenching was done right after the sonication was interrupted. **b** Sample 2, in which prolonged sonication was continues during thermal quenching

Table 1 Structural parameters of sample 1 obtained from the Rietveld refinement

	Bi Rhombohedral, R-3 m	Sn Tetragonal, $I4_1/amd$	Bi_2Sn Tetragonal, $I4_1/amd$	β′-Sn Tetragonal, $I4_1/amd$
Sample 1, $R_w = 9.8$				
a/Å	4.451 (2)	5.844 (2)	6.216 (2)	5.884 (2)
c/Å	11.86 (1)	3.186 (2)	3.319 (2)	3.202 (2)
<*D*>/Å	$>10^3$	$>10^3$	$>10^3$	$>10^3$
σ%	0.08 (1)	0.08 (1)	0.10 (1)	0.08 (1)
mass%	33.6 (5)	31.0 (5)	15.2 (2)	20.2 (3)
Sample 1 treated at 320 °C, $R_w = 4.7$				
a/Å	4.544 (2)	5.846 (2)	–	–
c/Å	11.88 (1)	3.188 (2)	–	–
<*D*>/Å	$>10^3$	$>10^3$	–	–
σ%	0.06 (1)	0.10 (1)	–	–
mass%	56.3 (5)	34.1 (5)	–	–

The agreement factors R_w are reported for each of the refinements. The number in round brackets indicates the uncertainly in the last digit and is referred to as an estimated standard deviation

out to form a periodic structure of lamellae with the solid Bi embedded in a matrix of the Sn solid phase. The limit of solubility of bismuth in tin, below the eutectic temperature, allows the formation of a heterogeneous alloy rather than single-phase solid solution. The unit cell parameters obtained for tetragonal Sn structure and for rhombohedral Bi structure by the Rietveld refinement show no substantial deviations from the expected values [21] and from XRD pattern of as-casted alloy (data not reported). The signals at 30.60° (2θ degrees), which overlaps with the Sn (200) plane, and at 28.75, 41.05, 42.40 and 43.50° (2θ degrees), all assigned to the metastable phase, are indexed in terms of a β-tin type structure rich in bismuth in which only one-third of tetragonal sites are occupied by Sn. The equilibrium Bi–Sn phase diagram at room temperature and pressure not provided this kind of supersaturated solid solution of bismuth in tin. For this reason, we deduce that this tetragonal structure rich in bismuth is a new phase that differs from Bi and Sn equilibrium phases.

The stoichiometry of this phase Bi_2Sn was determined by taking into account both the total amount of phases that contain or dissolve Bi, fitted by the Rietveld method, and the bismuth overall nominal composition (57 mass%). The peaks at 31.90, 43.50 and 44.60° (2θ) are slightly shifted with respect to the reflections of the main Sn phase and are indexed as tetragonal tin type structure (labeled as β′-Sn). The reflection positions of β′-Sn very close to those of Sn main phase are not reported in Fig. 2.

In the case of Bi_2Sn and β′-Sn phases, the cell parameters (*a* and *c*) differ from the β-Sn structure. It was found that their tetragonal unit cell is more stretched with a *c*/*a* axial ratio slightly smaller (in the undistorted β-Sn unit cell the *c*/*a* ratio is 0.546). In the case of the Bi_2Sn phase, the cell distortion is greater and is accomplished with a slight strain of the structure due to high Bi contents, taking into account the difference between Sn and Bi atom radius. In the case of the β′-Sn phase, we suppose that the lattice parameters increase due to the partial substitution of Sn by Bi atoms in the tetragonal Sn cell [1]. Indeed, we presume that the β′-Sn phase is merely a supersaturated β-Sn solid solution which contains a significant amount of dissolved bismuth and therefore slightly changes in the cell parameters of β′-Sn phase in comparison with β-Sn are observed. We exclude the possibility that the ultrasonic process causes a new Sn phase structure with lower symmetry. Indeed, for the observed β′-Sn phase, the *c*/*a* axial ratio is 0.544, very close to the typical value of tetragonal Sn $I4_1/amd$ structure [22].

The formation of metastable phases is the consequence of different events that took place when the acoustic energy was applied to the Bi–Sn molten alloy in the hot oil. The complex combination of the various parameters generates by cavitation and associated shock waves [16] promote the formation of metastable Bi–Sn phases. Irradiation of the system with acoustic energy causes dispersion of the molten metal into microscopic spheres [17], which are then exposed to extreme conditions of high pressures and temperatures and rapid cooling rates. It is well known that the formation of non-equilibrium phases in the Bi–Sn system occurs under high pressure and/or rapid undercooling conditions [9]. It was established in the literature that the metastable phase was formed from samples with Bi contents between 30 and 60 at% [4]. However, different metastable phases were obtained starting with different Bi–Sn composition and using different procedure (i.e., high pressure and/or undercooling) [4, 6, 8]. The Bi_2Sn phase

obtained in this work by ultrasonication is very similar (in term of d-spacing) to the M1 phase that was obtained by Ishihara et al. [4] via rapid solidification of Bi–Sn alloy droplet samples. Another similar phase was obtained by Bhattacharya et al. [9] via rapid undercooling, starting from the eutectic mixture. These authors reported that this metastable phase exists over a wide range of compositions, and they defined this phase as a tetragonal β-Sn solid solution with a large amount of Bi. Taking into consideration the similarities between the literature data [4, 9] and our results, the Bi-rich metastable phases obtained in the present work should be the undercooled phases. It should be considered that when the ultrasonic energy is applied to a melt at its liquidus temperature, some regions in the melt are superheated, while other regions are undercooled. At each region, the melt is subject to changes from undercooling to superheating at high frequencies. This extremely fast local heating and cooling is induced by the bubbles growth and collapse during the cavitation process. The rapidly solid–liquid transitions promote an increase in the amount of solid nuclei in the melt. The presence of numerous heterogeneous nucleation sites controls the metastable phase formation as described by Bhattacharya et al. [9]. Overall, during the solidification, the bismuth precipitates as the primary phase and the remaining Sn-rich liquid stays in equilibrium with Bi and follows the liquidus line of phase diagram. However, in some regions, a local metastable extension of the phase diagram is provided by the ultrasonication because it causes local temperature and composition variations and promotes the diffusion between liquid and solid nuclei. The Bi liquidus curve may cross the so-called T_0-line in the Sn-rich side and a large amount of bismuth may be entrapped in β-Sn structure [9].

According to Chen et al. [23], only Bi–Sn nanoparticles in the eutectic composition were observed by the ultrasonication process, and no metastable phase was evident in the XRPD pattern. This result can be explained by the slow cooling of the Bi–Sn system after the sonication, allowing it to reach the most stable state.

DSC analysis of sample 1 was done in the temperature range of 20–320 °C, at a scan rate of 10 °C min^{-1}. On the first heating scan, a small endothermic signal with an onset temperature of 115 °C was observed, followed by an intense sharp endothermic signal with an onset temperature of 137 °C. The former is attributed to the melting of the minor metastable phases Bi_2Sn and β′-Sn, while the latter is attributed to the melting of the eutectic Bi–Sn alloy. In addition, a broad endothermic band centered at 270 °C is observed. On the second heating scan, only the main signal for the melting of the eutectic alloy is observed, while the others have vanished, which can be interpreted as the conversion of the metastable phases into the stable Bi–Sn phase when the system was heated up to 320 °C. This explanation is supported by the increase in the $\Delta_m H$ on the second heating cycle (Table 2) and also by the XRD analysis of the sample after heating to 320 °C. The results of the Rietveld refinement show no signals for the two metastable phases but the appearance of a small signal for SnO (Romarchite, PDF card 06-0395), due to some oxidation at elevated temperatures. These results are somewhat different than those reported in Ref. 6 and 9, in which the signals for the metastable phases did not disappear. However, in those works, the systems were heated only up to 200 °C, which eventually was not high enough to induce phase transformation (Fig. 3).

Further investigation of the thermal behavior of the system was done by 10 min annealing of the sample at 127 °C, followed by XRD analysis. The XRD pattern showed that while the signals for Bi, Sn and Bi_2Sn were unchanged, the signals for the β′-Sn phase disappeared, which means that only one of the metastable phases, β′-Sn, decomposes at this temperature, while the other phases, Bi_2Sn, do not. DSC measurement of the annealed sample (Fig. 4) showed again the small signal starting at 115 °C, which can now be attributed solely to Bi_2Sn. The different shape of this signal, in comparison with the sharp melting signal of the eutectic alloy, can be explained from a kinetic point of view, due to the different rates of diffusion in melt of the Bi_2Sn and the eutectic alloys. This was observed for other systems containing different intermetallic compounds [24].

In order to investigate the ultrasonic effect on the evolution of new phases or transformation between phases, sample 2 was prepared in a similar manner, but the sonication was continued during the cooling of the sample to 110 °C. XRD analysis (Fig. 5) showed that the main phases were β-Sn with tetragonal structure and Bi with rhombohedral structure. Signals for the β′-Sn metastable phase were absent, but the Bi_2Sn tetragonal phase together with new reflections indicating the presence of a new metastable phase was identified. The results of the Rietveld analysis are summarized in Table 3.

The composition of the unknown new metastable phase was assessed from its lattice parameters (fitted by Rietveld) using the Vegard law [25]. Indeed, plotting the lattice parameters of pure Sn, BiSn and $Bi_{0.05}Sn_{0.95}$ (tetragonal

Table 2 Enthalpy values of melting for the sample 1 on the two consecutive heating cycles

	$\Delta_m H$/J g^{-1}	
	First peak (metastable phases)	Second peak (Eutectic phase)
First heating cycle	3.9 (1)	28.7 (6)
Second heating cycle	–	34.5 (7)

The number in round brackets indicates the uncertainly in the last digit and is referred to as an estimated standard deviation

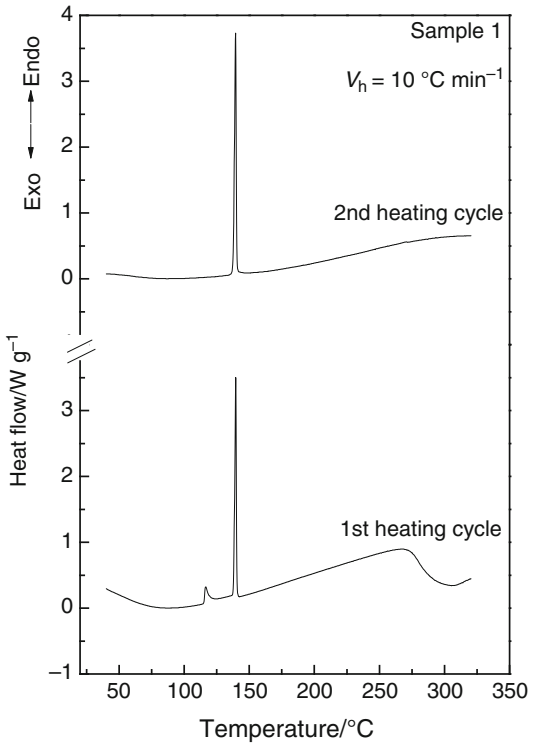

Fig. 3 DSC heating curves for sample 1

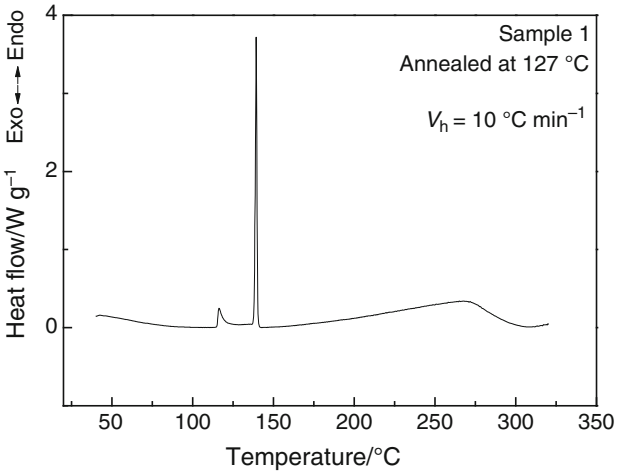

Fig. 4 DSC heating curve for the sample 1 previously annealed at 127 °C for 10 min and cooled at 200 °C min^{-1}

$I4_1/amd$) alloys versus the composition shows that the bismuth–tin system obeys the Vegard law for alloys which contain up to 50 at% Bi. The new metastable phase is indexed in term of a tetragonal tin type structure with equiatomic composition BiSn. The comparison between the X-ray diffraction peaks of this equiatomic metastable phase and those reported in literature suggests that the BiSn phase obtained in this work is be similar to the high-pressure phase reported by Boiko [3]. One of the most

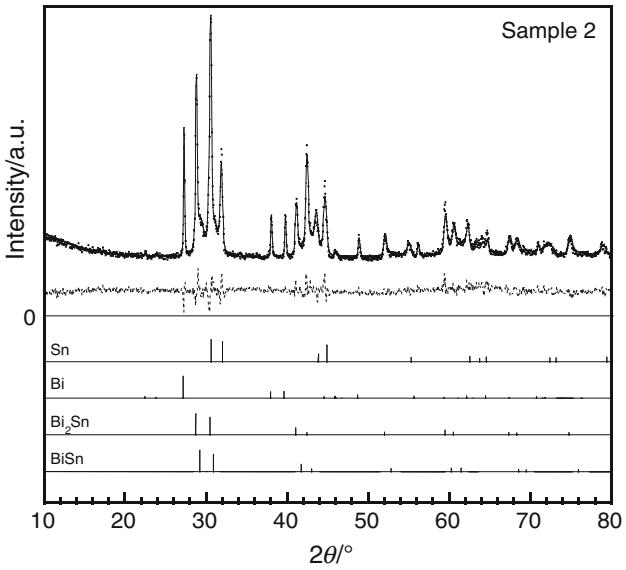

Fig. 5 Rietveld refinement for the sample 2. The *dots* are the experimental data, the *solid line* is the calculated data and the *dotted line* is the difference profile. *Lower vertical bars* represent reflection positions of Bi, Sn, Bi_2Sn and BiSn phases

plausible interpretations concerning the BiSn phase is that it is formed from the β′-Sn phase during the continuous sonication of the solidifying melt. The β′-Sn particles of 100 nm in diameter undergo energetic collisions that are generated by the shock waves and the microjects [17], and as a result, they melt and produce particles of BiSn equiatomic phase. It is noteworthy that the mean crystallite diameter for the BiSn phase is below 100 nm.

The lattice constants fitted for the BiSn phase are similar to those for the Bi_2Sn phase with *c*/*a* distortion within tetragonal structure due to the high contents of Bi. This distortion is common to very high microstrain values. In Table 3, the main Sn phase also presents a distorted tetragonal cell (due to the partial substitution of Sn by Bi atoms). This is suggested by both the lattice parameters being slightly higher, with respect to pure Sn, and by the slightly high value of microstrain. On the contrary, the lattice parameters for the Bi phase were approximately similar to those of pure Bi.

In comparison with sample 1 (Table 1), the mean crystallite size of the main Sn phase in sample 2 is smaller (Table 3). This can be due to the grain refinement caused by the prolonged sonication.

The thermal behavior of sample 2 was evaluated by DSC at ambient pressure. Figure 6 displays three consecutive heating cycles (the cooling curves are not shown). In the first cycle, two small endothermic peaks are seen at similar temperatures as appeared in Fig. 3, together with a wide signal centered at 250 °C. In this case, the first broad peak is attributed to Bi_2Sn and BiSn,

Table 3 Structural parameters of sample 2 obtained from the Rietveld refinement

	Bi Rhombohedral, R-3 m	Sn Tetragonal, $I4_1/amd$	Bi_2Sn Tetragonal, $I4_1/amd$	BiSn Tetragonal, $I4_1/amd$
Sample 2, $R_w = 9.9$				
a/Å	4.535 (2)	5.873 (2)	6.211 (2)	6.112 (2)
c/Å	11.87 (1)	3.199 (2)	3.320 (2)	3.279 (2)
<*D*>/Å	$>10^3$	533 (20)	$>10^3$	354 (20)
σ%	0.10 (1)	0.30 (3)	0.20 (2)	0.10 (1)
mass%	7.8 (2)	39.6 (1)	27.6 (1)	25.0 (1)
Sample 2 treated at 104 °C, $R_w = 4.5$				
a/Å	4.539 (2)	5.870 (2)	6.210 (2)	6.120 (2)
c/Å	11.88 (1)	3.200 (2)	3.318 (2)	3.287 (2)
<*D*>/Å	$>10^3$	532 (20)	$>10^3$	345 (20)
σ%	0.10 (1)	0.40 (3)	0.20 (2)	0.10 (1)
mass%	13.3 (1)	40.1 (1)	18.3 (1)	28.3 (1)
Sample 2 treated at 145 °C, $R_w = 3.1$				
a/Å	4.541 (2)	5.881 (2)	6.223 (2)	6.118 (2)
c/Å	11.88 (1)	3.202 (2)	3.323 (2)	3.287 (2)
<*D*>/Å	$>10^3$	532 (20)	$>10^3$	392 (20)
σ%	0.10 (1)	0.20 (2)	0.20 (2)	0.10 (1)
mass%	10.5 (2)	39.4 (1)	19.3 (1)	30.8 (1)
Sample 2 treated at 200 °C, $R_w = 2.1$				
a/Å	4.536 (2)	5.873 (2)	6.212 (2)	6.113 (2)
c/Å	11.88 (1)	3.200 (2)	3.320 (2)	3.283 (2)
<*D*>/Å	$>10^3$	420 (20)	$>10^3$	392 (20)
σ%	0.10 (1)	0.30 (3)	0.30 (3)	0.10 (1)
mass%	11.0 (2)	41.7 (1)	20.2 (1)	27.1 (1)
Sample 2 treated at 275 °C, $R_w = 2.4$				
a/Å	4.544 (2)	5.846 (2)	6.206 (2)	6.085 (2)
c/Å	11.88 (1)	3.186 (2)	3.324 (2)	3.275 (2)
<*D*>/Å	$>10^3$	$>10^3$	$>10^3$	200 (20)
σ%	0.06 (1)	0.10 (1)	0.30 (3)	0.02 (1)
mass%	27.2 (1)	37.9 (1)	15.6 (1)	17.1 (1)
Sample 2 treated at 320 °C, $R_w = 1.9$				
a/Å	4.545 (2)	5.860 (2)		
c/Å	11.90 (1)	3.193 (2)		
<*D*>/Å	$>10^3$	534 (20)		
σ%	0.10 (1)	0.010 (1)		
mass%	54.4 (1)	40.5 (1)		

The agreement factors R_w are reported for each of the refinements. The number in round brackets indicates the precision in the last digit and is referred to as an estimated standard deviation

and the second sharp peak to the eutectic alloy. However, on the second and third heating cycles, only an intense signal is observed which can be attributed to the melting of the eutectic alloy. This result suggests again that during the first heating scan up to 320 °C, the metastable phases decompose into the equilibrium phases, as indicated by the values of $\Delta_m H$ in Table 4. After first heating at 320 °C, the area under the eutectic peak increases at the expense of the metastable phases. However, the intensity of the endothermic peak for the eutectic phase decreases in the third cycle due to oxidation of some of the sample. In the second and third cycles, a slightly endothermic peak is observed around 270 °C which was related to a portion of the Bi that does not participate in the eutectic melting and that has the tendency to superheat. This behavior of the bismuth was observed by also Bhattacharya et al. using the high-temperature X-ray diffraction technique [9].

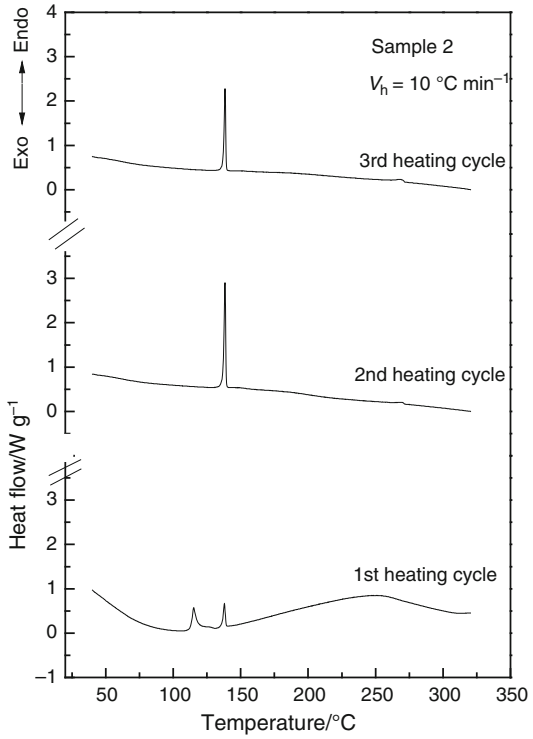

Fig. 6 DSC curves for sample 2, showing the three consecutive heating cycles

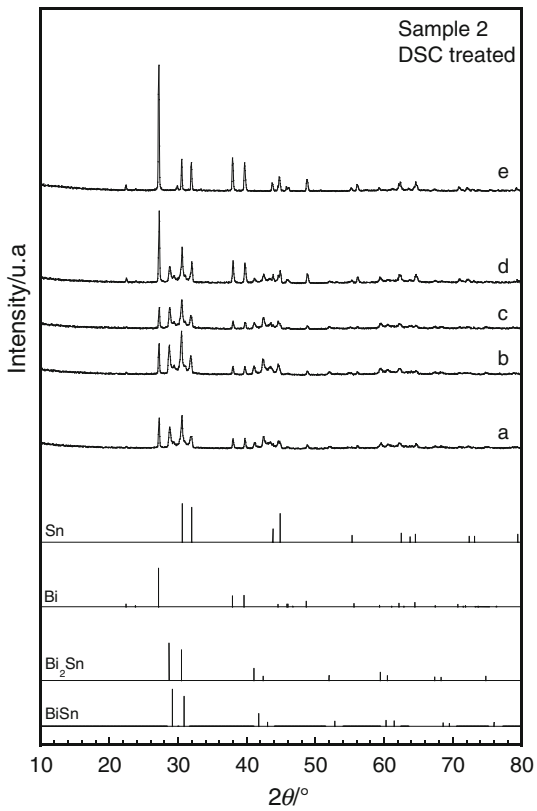

Fig. 7 XRPD patterns of several portions of sample 2 which were thermally treated at the following temperatures: *a* 104; *b* 145; *c* 200; *d* 275 and *e* 320 °C

Table 4 Enthalpy values of melting for the sample 2 on the three consecutive heating cycles

Sample 2	$\Delta_m H$/J g^{-1}	
	First peak (metastable phases)	Second peak (Eutectic phase)
First heating cycle	14.3 (2)	5.9 (1)
Second heating cycle	–	20.9 (2)
Third heating cycle	–	15.5 (2)

The number in round brackets indicates the uncertainly in the last digit and is referred to as an estimated standard deviation

In order to get a better insight of the thermal-induced phase transformation, portions of sample 2 were treated at several temperatures under Ar atmosphere and examined by XRD. The diffractograms are presented in Fig. 7. The selected temperatures were chosen on the basis of the first heating cycle for this sample (Fig. 6).

The lower vertical bars represent the reflection positions of Bi, Sn, Bi_2Sn and BiSn phases.

The diffractograms shows do not exhibit differences among the samples that were heated at 104, 145 and 200 °C. Only at 275 °C, some changes can be observed, i.e., progressive lowering of the reflections intensities belonging to the metastable phases. In the sample that was heated to 320 °C, the dominant phases are Bi and Sn, while the signals for the Bi_2Sn and BiSn metastable phases disappeared. The quantitative analysis of the diffraction data in Fig. 7 was carried out by Rietveld method, and the results are listed in Table 3.

The sample heated at 104 °C reveals a few changes with respect to sample 2 which was not thermally treated. A slight increase in the content of the Bi, Sn and BiSn phases compensated for the reduction in Bi_2Sn phase contents, suggesting that in the temperature range of 20–104 °C, before melting starts, a small fraction of Bi_2Sn phase is involved to a decomposition. It can be deduced that a portion of Bi_2Sn particles are not stable at low temperature and decompose into Bi, Sn and BiSn below their melting temperature. In the sample treated at 145 °C, a slight reduction in Bi and Sn phase contents is observed, whereas the content of the Bi_2Sn and BiSn phases slightly increased. This result shows that near the melting point the fraction of metastable phases is enhanced, whereas that for the eutectic phase decreases.

In the sample treated at 200 °C, reduction in BiSn phase content is observed with respect to the sample treated at 145 °C. This reduction is associated with the corresponding increase in Sn, Bi and Bi_2Sn.

It should be noted that in all the samples that were treated at temperatures up to 200 °C, the Sn, Bi_2Sn and BiSn phases showed a tetragonal structure with slightly microstrain, but substantial variations in cell parameters are observed. Heating at 275 °C resulted in lower content of BiSn and Bi_2Sn as a consequence of a partial decomposition. The bismuth fraction in the products increased from 11 to 27.2 mass%. This is due both to decomposition of the metastable phases and release from main Sn phase of dissolved Bi. The Sn phase shows a lower microstrain value indicating a lesser lattice stress accordingly to bismuth demixing. In that sample, a small amount of the SnO (about 2 mass%) was observed as a result of some oxidation. The metastable phases disappeared completely after heating at 320 °C, and the content of Bi and Sn was found to be 55 and 45 mass%, respectively, in good agreement with the initial stoichiometric composition (Bi 57 and Sn 43 mass%). These results show that the metastable phases decompose in the range 200320 °C into the equilibrium components β-Sn and rhombohedral Bi. In the sample treated at 320 °C, the amount of the SnO is about 5 mass%.

Conclusions

Ultrasonic irradiation of the molten eutectic $Bi_{43}Sn_{57}$ alloy induces the formation of two BiSn metastable phases. Their composition and structure were determined by XRPD using the Rietveld refinement. These metastable phases are similar to high undercooling phases or high-pressure phases that were reported in the literature. The XRPD study reveals that these metastable phases are bismuth-rich β-Sn type tetragonal structures. The DSC heating curve showed the melting of the metastable phases in addition to the melting of the eutectic phase. It was shown that in the range 200–320 °C, the metastable phases convert irreversibly to the equilibrium components. When the sonication was applied during the cooling stage, transformations of the metastable phases were observed.

Acknowledgements This research is a contribution to the European COST Action MP0903 "Nanoalloys as advanced materials: from structure to properties and applications". The authors would like to thank the LR.2007 Regione Autonoma della Sardegna for financial support (LR.7/2007 Project No. F71J11001220002-year 2010).

References

1. Braga MH, Vizdal J, Kroupa A, Ferreira J, Soares D, Malheiros LF. The experimental study of the Bi–Sn, Bi–Zn and Bi–Sn–Zn systems. Calphad. 2007;31:468–78.
2. Vizdal J, Braga MH, Kroupa A, Richter KW, Soares D, Malheiros LF, Ferreira J. Thermodynamic assessment of the Bi–Sn–Zn system. Calphad. 2007;31:438–48.
3. Tonkov EY. Compounds and alloys under high pressure: a handbook. Boca Raton: CRC Press; 1998. p. 584.
4. Ishihara KN, Maeda M, Mori K, Shingu PH. Metastable phase diagram of the Sn–Bi system. Int J Rapid Solidif. 1987;3:11–22.
5. Da Silveira AF, de Castro WB, Luciano BA, Kiminami CS. Microstructure of under-cooled Sn–Bi and Al–Si alloys. Mater Sci Eng A. 2004;375–377:473–8.
6. Yoon W, Perepezko JH. The effect of pressure on metastable phase formation in the undercooled Bi–Sn system. J Mater Sci. 1988;23:4300–6.
7. Kane RH, Giessen BC, Grant NJ. New metastable phases in binary tin alloy systems. Acta Metall. 1966;14:605–9.
8. Wang N, Wei B. Rapid solidification behaviour of Ag–Cu–Ge ternary eutectic alloy. Mater Sci Eng A. 2001;307:80–90.
9. Bhattacharya V, Yamasue E, Ishihara K, Chattopadhyay K. On the origin and stability of the metastable phase in rapidly solidified Sn–Bi alloy particles embedded in Al matrix. Acta Mater. 2005;53:4593–603.
10. Corrias A, Ennas G, Marongiu G, Paschina G. Solid-state reaction induced by milling of a mixture of cobalt and boron powders. J Mater Sci. 1991;26:5081–4.
11. Zhang P, Crespi V, Chang E, Louie S, Cohen M. Theory of metastable group-IV alloys formed from CVD precursors. Phys Rev B. 2001;64:235201.
12. Espiritu RD, Amorsolo AV. DSC analysis of Cu–Zn–Sn shape memory alloy fabricated via electrodeposition route. J Therm Anal Calorim. 2011;107:483–7.
13. Frongia F, Pilloni M, Scano A, Ardu A, Cannas C, Musinu A, Borzone G, Delsante S, Novakovic R, Ennas G. Synthesis and melting behaviour of Bi, Sn and Sn–Bi nanostructured alloy. J Alloys Compd. 2015;623:7–14.
14. Suslick KS, Choe S-B, Cichowlas AA, Grinstaff MW. Sonochemical synthesis of amorphous iron. Nature. 1991;353:414–6.
15. Li Q, Li H, Pol VG, Bruckental I, Koltypin Y, Calderon-Moreno J, Novik I, Gedanken A. Sonochemical synthesis, structural and magnetic properties of air-stable Fe/Co alloy nanoparticles. New J Chem. 2003;27:1194–9.
16. Suslick KS, Didenko Y, Fang MM, Hyeon T, Kolbeck KJ, McNamara WB III, Mdleleni MM, Wong M. Acoustic cavitation and its consequences. Philos Trans R Soc A. 1999;357:335–53.
17. Friedman H, Reich S, Popovitz-Biro R, von Huth P, Halevy I, Koltypin Y, Gedanken A, Porat Z. Micro- and nano-spheres of low melting point metals and alloys, formed by ultrasonic cavitation. Ultrason Sonochem. 2013;20:432–44.
18. Kumar VB, Gedanken A, Kimmel G, Porat Z. Ultrasonic cavitation of molten gallium: formation of micro- and nano-spheres. Ultrason Sonochem. 2014;21:1166–73.
19. Lutterotti L, Matthies S, Wenk HR. MAUD: a friendly Java program for material analysis using diffraction. IUCr Newslett CPD. 1999;21:14–5.
20. Young R. The Rietveld method. Oxford: Oxford University Press; 1993.
21. The International Centre for Diffraction Data—ICDD, JCPDF-2 database.
22. Salamat A, Briggs R, Bouvier P, Petitgirard S, Dewaele A, Cutler ME, Corà F, Daisenberger D, Garbarino G, McMillan PF. High-pressure structural transformations of Sn up to 138 GPa: angle-dispersive synchrotron X-ray diffraction study. Phys Rev B. 2013;88:104104.
23. Chen H, Li Z, Wu Z, Zhang Z. A novel route to prepare and characterize Sn–Bi nanoparticles. J Alloys Compd. 2005;394:282–5.
24. Ciulik J, Notis MR. The Au–Sn phase diagram. J Alloys Compd. 1993;191:71–8.
25. Vegard L. Die Konstitution der Mischkristalle und die Raumfüllung der Atome. Zeitschrift für Phys. 1921;5:17–26.